Atmos. Chem. Phys. Discuss., 0000, 0001–**??**LastPage, 2008
www.atmos-chem-phys.org/acpd/0000/0001/
SRef-ID: 1680-7375/acpd/2008-0000-0001
European Geosciences Union

LOGO

2003 Canberra megafires: impact on tropospheric ozone & aerosols

G. Guerova[1] **and N. Jones**[1]

[1]Centre for Atmospheric Chemistry, University of Wollongong, Wollongong, NSW 2522, Australia

Received: – Accepted: – Published:

Correspondence to: guergana@uow.edu.au

Abstract

2003 was a record year for wildfires worldwide. Severe forest fires killed four people, displaced 20,500 others and burnt 260,000 ha around Canberra, Australia in January 2003. The uncontrolled fires ignited in early January 2003 are a result of a prolonged El Niño drought in south-east Australia. Severe weather conditions resulted in a fast spread of the fires and poor air quality in a region where 70% of the population of Australia leaves. In Victoria, the air quality 4-hour ozone (O_3) standard exceedences are reported on 17th, 24th and 25th January. We use the state-of-art global chemistry and transport model GEOS-Chem in conjunction with ground and space based observations to study the O_3 and aerosol enhancement due to bushfires. Firstly, the monthly mean surface O_3 and Aerosol Optical Depth (AOD) in January 2003 are compared to January 2004 and secondly, from sensitivity model simulations, four episodes are isolated and an attempt is made to quantify the contribution of the bushfires on the air quality on the metropolitan areas in the states of Vic and SA.

In January 2003 the observed monthly mean afternoon surface O_3 in south-east Australia reached 27.5 ppb, which is 6.5 ppb (i.e. 30%) higher than in 2004. The simulated O_3 is 29.5 ppb which is 10 ppb higher than in 2004. While the model tends to overestimate the observed O_3 concentrations it exhibits a very good skill in reproducing the O_3 temporal variability in January 2003 with a correlation of 0.81. Thus the model sensitivity simulations can be used to select and study the major bushfire episodes when the bushfire air masses reach the metropolitan areas of Vic and SA. On 12, 17, 24-25 and 29 January 2003, the observed O_3 peaks above 40 ppb and the simulated bushfires contribution is higher that 10 ppb. During these 4 episodes the range of observed O_3 enhancement due to bushfires is 20-35 ppb, which is a factor of 3 to 5 higher than the monthly mean. The simulated bushfire O_3 enhancement is in the range 15-50 ppb with a factor of 1.5 to 5 higher than the monthly mean. During two episodes, a well formed surface wind channel stretches across the Tasman Sea facilitating the long range transport to New Zealand.

During the four episodes in January 2003 the AOD reached 0.5 with the simulated and observed AODs in good agreement on the spatial structure. The model shows a tendency to underestimate the AOD, but proves a useful tool for reconstruction of the mostly patchy observed MODIS AODs. As the AOD represent the load in the troposphere it also reflects the faster transport in the free troposphere and the AOD enhancements are seen about a day ahead from the surface O_3 enhancement.

1 Introduction

The biomass burning has a major contribution to the emissions of tropospheric trace gasses and aerosols. According to Giglio et al. (2006) in the period 2001-2004 the total area burned in Africa and Australia comprised 80% of the area burned globally. Biomass burning in Australia occurs in two major regions: a.) the tropical region in northern Australia with the savanna type vegetation of grass and shrubs with relatively low fuel loads but extensive area burned and b.) south-east Australia, the states of South Australia (SA), Victoria (Vic), New South Wales (NSW) and Australian Capital Territory (ACT), predominantly covered with eucalyptus forests with high fuel loads and relatively low area burned. South-east Australia has the reputation to be one of the tree most fire-prone regions globally, along with southern California and southern France (Hennessy et al., 2005). The region has high population density with 70% (i.e. 13.8 million), of the 20 million population of Australia, leaving in these states. With an estimate of emissions associated with wild forest fires being factor of 4 higher than savanna burning the air quality can be an issue during the biomass burning season, provided the air mass reaches the populated coastal regions. This study will cover the surface ozone (O_3) enhancement and aerosol loading during the devastating magafires in January 2003, which displaced 20 500, burnt 260 000 ha in Vic, NSW and ACT.

The 2002-2003 bushfire season in south-east Australia occurred during an on-going drought that is one of the most severe in recorded history with the first bushfires occurring early in the season in September 2002. The drought is associated with El Niño warm phase that caused prolonged rainfall deficiencies on the east coast of Australia for the six months to January 2003 with only half of the rainfall recorded in the period July to December (Taylor and Webb, 2005), (Leslie and Speer, 2006). In January 2003 the monthly mean temperature was about 1°C above average and in Vic and NSW it reached 2-3°C. In addition the temperature from April to January was significantly above the average with November 2002 the maximum monthly mean temperature 5°C above the average (Taylor and Webb, 2005). High temperature and low rainfall facili-

tated the curing of both of fine and heavy fuel prior to January 2003 thus abundance of dry fuel primed for burning. Taylor and Webb (2005) discuss in great detail the synoptic and local conditions associated with the devastating fires in January 2003 and point out that the wildfire activity initiated by lightening in Vic and NSW on 7-8 January that was not completely brought under control until early March. The interplay of warm to hot air, low humidity in the evening and strong winds associated with a strong frontal system moving through the south-east of the continent facilitated the spread of fire (Taylor and Webb, 2005). Ultimately, high lightning activity and extreme fire weather days led to the ignition and rapid spread of a number of large unplanned fires and economic damage estimate of around 354 million $ in terms of loss of dwellings (over 500 in Canberra on 18 January), buildings and stock.

Concentrations of O_3 in clean surface air are in the range 5-30 ppbv (Jacob, 1999). The surface O_3 is toxic to humans and vegetation because it oxidises biological tissue. O_3 is produced in the troposphere from the oxidation of $CO$and hydrocarbons in the presence of NO_x. In densely populated regions with high emissions of NO_x and hydrocarbons, rapid O_3 production can take place and result in a surface air pollution problem in the Northern Hemisphere. In the Southern Hemisphere O_3 is produced during biomass burning which is the second largest NO_x and CO emission source globally. Atmospheric aerosols have natural as well as anthropogenic sources. Natural sources include wind-blown dust, sea salt, large-scale dust storms, naturally occurring forest fires, and volcanic eruptions. Anthropogenic aerosols are primarily from emissions from motor vehicles, industries, power plants, and biomass burning due to agricultural practices.

The Australian urban areas are more susceptible to photochemical smog because of local meteorological conditions, higher solar radiation, and emission of local pollutants (Manins, 2001). Sydney is a classic closed basin, bounded by high-altitude land to the south, west, and north, and pollution may accumulate and circulate inside the city for several days, exacerbated by relatively frequent temperature inversions (Gupta et al., 2007). Gupta et al. (2006) report that the air-quality conditions in Sydney during

bushfire events are comparable to the conditions in highly polluted cities such as Hong Kong and New Delhi. Due to a limited number of ground stations, it is very difficult for the local agencies to provide air-quality alerts over large spatial scales during major bushfire events.

This paper is organized as follows: section 2 presents the datasets used; the GEOS-Chem model setup is presented in section 3; section 4 gives a summary of the temporal and spatial variability of O_3 and AOD in January 2003 and 2004; a deteiled study of four episodes in January 2003 is available in section 5; and conclusions are given in section 6.

2 Observation datasets

2.1 Aerosol optical depth from MODIS

Terra and Aqua are polar orbiting satellites of the NASA Earth Observing System (Salomonson et al. (1989), King et al. (1992), King et al. (2003)) which carry Moderate Resolution Imaging Spectroradiometer (MODIS) instruments that take global Aerosol Optical Depth (AOD) observations twice daily. MODIS spatial resolution is 250 m at nadir, has 2330 km wide swath, and spectral range in 36 channels, 7 of which are dedicated for aerosol retrieval (470, 550, 650, 850, 1240, 1650 and 2130 nm). We use the Level-2 product with 10 km resolution available through the LAADS web (http://ladsweb.nascom.NASA.gov/data/) that is averaged to GEOS-Chem resolution of 2° latitude by 2.5° longitude.

MODIS AOD products over the ocean are generally unbiased with low uncertainty (Remer (2002), Levy et al. (2005)), but the land AOD products are subject to higher uncertainty and a persistent high bias (Ichoku et al. (2002), Kinne (2003), Chin et al. (2004), Matsui et al. (2004), Abdou et al. (2005), Levy et al. (2005)).

2.2 Surface observations EPA

We use data from Environment Protection Authority (EPA) air quality monitoring networks of SA, Vic and NSW. The NSW air quality monitoring program collects real-time measurements of ambient level pollutants at over 24 monitoring stations located around the greater metropolitan area of Sydney, the Illawarra, the Lower Hunter and selected rural sites around NSW (http://www.environment.nsw.gov.au/air/airdata.htm). Of these 15 residential and 3 rural stations report O_3 concentrations. The EPA Victoria operates O_3 air quality monitoring in 11 residential and 4 rural stations (http://www.epa.vic.gov.au/air/bulletins/airmonlc.asp). In 2003 O_3 exceeded the standards in 5 days which is more frequent than in recent years. In January 2003 O_3 exceedences of the 1-hour (100 ppb) and 4-hour (80 ppb) standards are reported on the 17th, 24th and 25th (Victoria, June 2004). Each of the exceedences occurred during the bushfires burning in Victoria and New South Wales. South Australia EPA operates the air quality network with 4 O_3 monitoring sites in the metropolitan area of Adelaide (http://www.epa.sa.gov.au/index.html). In 2003, one-hour averages of ozone at three sites (Netley, Kensington and Northfield) were within the range 0-74 ppb. There were no exceedences of the 4-hour standard in South Australia in January 2003 (Australia, June 2004).

3 Model description

The global three-dimensional chemistry and transport model GEOS-Chem, version 7-04-11 with a horizontal resolution of 2° latitude by 2.5° longitude and 30 vertical levels from the surface to 0.01 hPa (http://www.as.harward.edu/chemistry/trop/geos/), is used in this work. The model is driven by the NASA Global Circulation Model GEOS-4 with a temporal resolution of 3 and 6 hours. Online chemistry with 43 tracers provides a comprehensive description of the NO_x-O_x-hydrocarbon chemistry and of tropospheric aerosols, which include nitrate-ammonium-sulfate aerosols, mineral dust, sea salt, black and organic carbon, and secondary organic aerosols. A total of 350 chemi-

cal reactions are taken into account in the chemical mechanism for 90 different species, as described in Park et al. (2004). The photolysis rates are calculated with the Fast-J algorithm which accounts for clouds and aerosols (Wild and Akimoto, 2001). Dry deposition velocities are computed following Wesely (1989) and Wang et al. (1998). Wet deposition is applied to gases, dust and hydrophilic aerosols as described in Liu et al. (2003).

Anthropogenic emissions of NO_x, CO, SO_2 are from EDGAR3.2, the hydrocarbons and sulfur are from the Global Emissions Inventory Activity (GEIA) for 1985 (Benkovitz et al., 1996) with updated national emissions inventories and are scaled for specific years (Bey et al. (2001) Park et al. (2004)). Over Europe, North America and northern Mexico, anthropogenic NO_x, CO, hydrocarbon and sulfur emissions are taken from the European Monitoring and Evaluation Program (EMEP) for the year 2000, (Auvray and Bey, 2005) the EPA National Emissions Inventory (NEI99) for the year 1998 and BRAVO. Anthropogenic emissions for NO_x and CO over Asia are from Streets et al. (2003) and Streets et al. (2006). Biomass burning emissions are from the Global Fire Emissions Database GFED2, (van der Werf et al., 2006) and biogenic emissions are calculated online using the MEGAN algorithm described by Guenther et al. (2006). Included are also aircraft and lightening NO_x and ship SO_2 emissions. Soil NO_x emissions are computed following Yienger and Levy (1995) with canopy reduction factors described by Wang et al. (1998).

Presented here are the results from a standard simulation that follows the set up described above for January 2003 and 2004 obtained after a one-year spin-up. Sensitivity simulations were conducted with biomass burning emissions turned off successively. Subtraction of the results from the sensitivity simulation from those of the standard simulation allows us to quantify the fraction of O_3 as solely a result of a specific O_3 precursor source. Due to non-linearity in the O_3 tropospheric chemistry, one has to be cautious when interpreting the results of the sensitivity simulations.

For the intercomparison with EPA observation the model data is sampled every two hours from which the afternoon daily and monthly means are computed.

4 Australian bushfires: January 2003 versus January 2004

4.1 Surface ozone and aerosol enhancement

Figure 1 presents the January 2003 fire hotspots detected by the ATSR sensor (http://dup.esrin.esa.int/ionia/wfa/index.asp) on board of the European Space Agency satellite. Clearly visible is the hotspot arc in Victoria and New South Wales. During 2002-2003 forest burning peaked in January 2003, which is about one month later compared to the other years. The model simulations in January 2003 show a large surface O_3 enhancement over south-east Australia (red spot in fig. 2a) and the monthly mean reaches 50 ppb. In comparison the monthly mean surface O_3 in January 2004 (fig. 2b) is about 30 ppb. Similarly, the aerosol loading is roughly doubled in January 2003 (fig. 2c) when compared with January 2004 (fig. 2d).

GEOS-Chem has been the subject of numerous global and regional evaluations that demonstrate the model skill in reproduction of the general features of tropospheric chemistry. The model has been previously the subject of several global evaluations (Bey et al. (2001), Martin et al. (2003) and Park et al. (2004)). However, this is a first study focused on Australia, thus the model evaluation is presented in table 1 using the surface O_3 observations from the three large east coast states SA, Vic and NSW. In

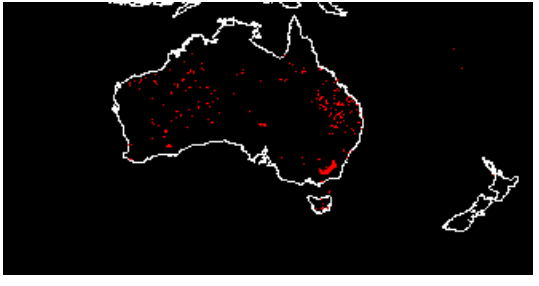

Fig. 1. ATSR fire hotspots over Australia in January 2003.

Year	2003	2004	Change
GEOS-Chem [ppb]	41	23	17
EPA [ppb]	28	26	2
GEOS-Chem NSW	65	30	33
EPA NSW	33	37	-4
GEOS-Chem Vic	32	19	12
EPA Vic	25	20	5
GEOS-Chem SA	27	19	8
EPA SA	30	22	8

Table 1. Afternoon (12-18 AEDT) monthly mean O_3 in January 2003 (column 2) and 2004 (column 3). The difference between 2003 and 2004 is given in column 4.

January 2003, the simulated monthly mean surface O_3 across the three states reaches 41 ppb, which is about 17 ppb higher that in January 2004. The observed surface O_3 in January 2003 is 28 ppb, which is about 2 ppb higher than in 2004. The large differences between model and observations are attributed to a factor of two overestimation in the simulated O_3 in NSW. This discrepancy will be further addressed in section 5. Note, that in Victoria and South Australia the simulated and observed concentrations agree within 7 ppb in 2003 and 3 ppb in 2004, thus the impact of bushfires will be quantified in those two states only. The bushfire contribution to the monthly mean afternoon O_3 consentartion in January 2003 is estimated to be in the range 8-12 ppb (column 4 in table 1), which is an increase of 30%.

When comparing the O_3 concentrations in 2003 (fig. 2a) and 2004 (fig. 2b) a clear O_3 enhancement in the range of 20-30 ppb is seen over central Australia. Note that, similar O_3 concentrations are seen in the capital cities of New South Wales and Victoria in January 2004. This is an arid region sparsely populated, with no major industrial activities and sparse vegetation cover. Using model sensitivity simulations we will track

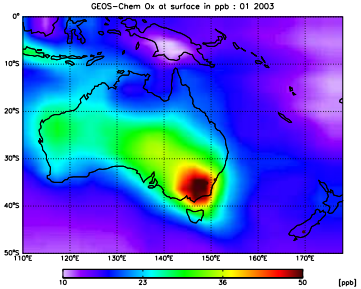

a.)

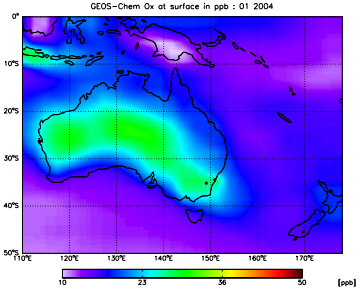

b.)

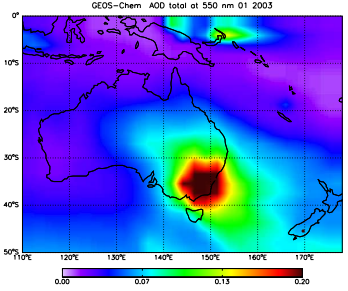

c.)

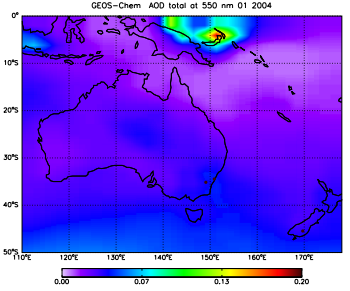

d.)

Fig. 2. Illustration of: a.) Surface ozone from GEOS-Chem: monthly mean January 2003, b.) Surface ozone from GEOS-Chem: monthly mean January 2004, c.) AOD at 500 nm from GEOS-Chem: January 2003 and d.) AOD at 500 mn from GEOS-Chem: January 2004.

the source of this enhancement in section 4.3. Note the AOD load is larger in 2003 (fig. 2c) that in 2004 (fig. 2d).

4.2 Temporal variation of surface ozone

In order to test the model skills in reproducing the temporal variation of afternoon (1200 – 1800 AEDT) surface O_3 in January 2003, the EPA observations from Victoria and South Australia are plotted against the simulated concentrations (solid grey line in fig.3). Several features stand out: i.) a very good correlation (r = 0.81) between observed and simulated ozone concentrations; ii.) six distinct episods when the observed daily averaged surface O_3 reached 40 ppb, 2 in the first half of the month and 4 in the second half; and iii.) overestimation of the simulated O_3 concentrations during 3 episods namely on 12, 17 and 24 January. In order to gain an insight for a possible reason for the model overestimation during these episods we examined the observed O_3 concentrations in 15 stations in Victoria. On 12 January 2003, the observed concentrations are in the range 16 - 66 ppb. 10 out of 13 stations reported concentrations above 40 ppb and 3 stations below 40 ppb. Similarly, on 17 January 2003 the observed O_3 is in the range 21 - 89 ppb and 9 out of 15 stations reported concentrations above 40 ppb. In one station only the O_3 exceeded the 4-hour standard of 80 ppb. On 24 January 2003, 10 out of 15 stations reported O_3 concentrations above 40 ppb and the range is 17-80 ppb. Thus it can be concluded that during this event the observed spatial variability in surface O_3 is not well captured by the model which is to be expected considering the coarse model resolution. Nonetheless, the simulated surface ozone consentrations are in the upper end of the observed variability.

Model sensitivity simulations are used to identify the major bushfire episodes. An episode is classified as major provided the O_3 due to bushfire (dashed gray line in fig. 3) is above the 10 ppb, a threshold inferred in section 4.1. Four episodes satisfy this condition, one during the first half of the month (12 January) and three in the second half (17, 24 and 29 January 2003). The episode on January 29 is well simulated thus the contribution of the fires can be inferred to be 15 ppb. Note, however, that on this day the observed O_3 concentration is in the range 38-74 ppb with 14 out of 15 stations in Victoria report concentration above 40 ppb. If we assume that the station reporting

the lowest concentration is representative for a clean air environment and the station reporting the maximum ozone enhancement represents the polluted air environment then the difference gives O_3 enhancement of 36 ppb. This is roughly double the one obtained from model sensitivity simulation. Application of this method for the remaining three events will help to quantify the impact of bushfire. For the episode on 24 January the observed versus simulated O_3 enhancement is 63 ppb versus 50 ppb. For the second episode on 17 January the difference in the observed O_3 is 68 ppb versus 25 ppb simulated. For the first episode on 12 January the observed O_3 enhancement is 50 ppb versus 40 ppb from the simulation. The feasibility of this approach will be assessed in section 5 via analysis of the weather regimes.

4.3 Sensitivity simulations

The model sensitivity simulations are used to deduce the bushfire impact on surface ozone in January 2003 (fig. 4a) and 2004 (fig. 4b). During January 2003, between 20 to 50 % of the ozone formation in south-east Australia comes from the bushfires. Some 10 % of the surface O_3 in central Australia and New Zealand can be attributed to the fires. In contrast during January 2004 the fire contribution is negligible. Note, however, that the enhanced O_3 over central Australia, reported in section 4.1, occured in both years thus it can be ruled out to only be due to bushfires.

To further explore the O_3 enhancement over central Australia, presented are the monthly mean surface winds from GEOS-Chem in January 2003 (fig. 4c) and 2004 (fig. 4d). From careful examination of the atmospheric circulation the following features can be identified: i.) prevailing westerly flow between 40 and 50° S; ii.) prevailing southerly flow on the west coast of Australia; iii.) anti-cyclonic curvature of the winds, well expressed in 2004 and less well in 2003, along the south coast of Australia between 30 and 40° S; iv.) south, south-westerly to westerly flow over central Australia. Note, that a common feature in both 2003 and 2004 is anti-cyclonic flow curvature over south-east Australia, between the Adelaide and Melbourne (black dots in fig. 4c and d). This suggests that the region is probably the source of pollution that is further advected

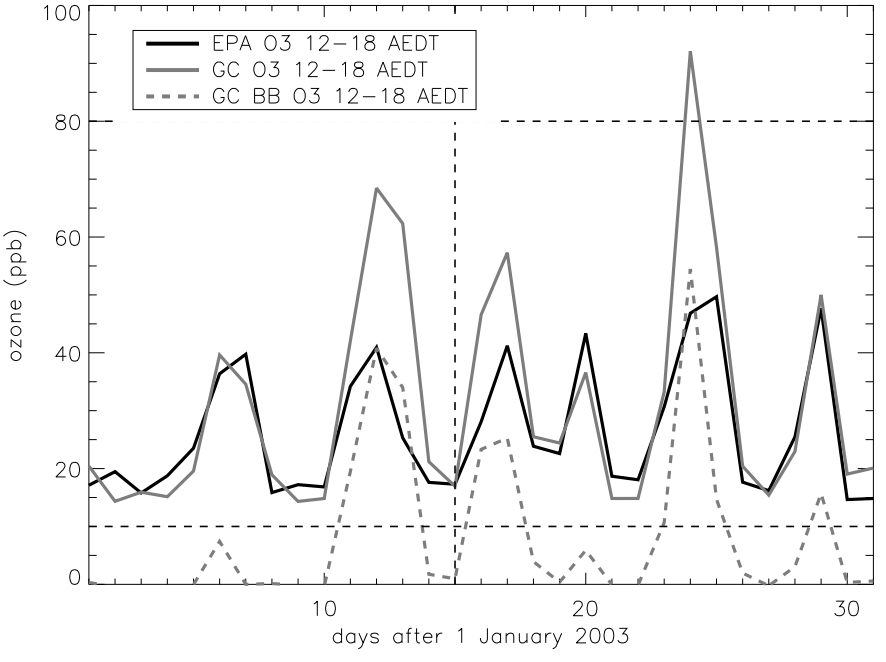

Fig. 3. Temporal variability of surface ozone over South Australia and Victoria from GEOS-Chem (solid grey line) and EPA (solid black line). Dashed gray line presents the biomass burning contribution obtained from GEOS-Chem sensitivity simulation.

to central Australia, thus the reported enhancement. In addition, in both fig. 2a and fig. 2b a distinct O_3 enhancement is seen north of Perth (black dot in fig. 4c) in both 2003 and 2004 and the prevailing wind supports the possible advection scenario. Further sensitivity simulations and observations will be necessary to confirm those findings which will be a subject of a future work.

5 Canberra magafire case studies

The identified in section 4.2 four major bushfire episodes (ES) in January 2003 are summarised in table 2 and discussed in detail below.

5.1 Episode I: 12 January 2003

The weather regime on 12 January is characterised by an anticyclone in the Tasman Sea. Well seen in fig. 5b is that over south-east Australia the wind turn from east (E) to north-east (NE). As to be expected, the bushfire air masses reach the metropolitan areas of Melbourne in Victoria, Adelaide in South Australia and over the Southern Ocean (fig. 5a). The observed maximum surface O_3 enhancement in Victoria reaches 66 ppb while the simulated is 70 ppb. It is to be noted that in Victoria both the model and the observation show a well pronounced west-east gradient in the O_3 concentrations, i.e. 40-50 ppb to the west and 10-20 ppb to the east. This is an indication about regional differences and suggests that the large variability in the observed O_3 concentrations are driven by two distinct air masses: one from the bushfires and one from the clean Tasman Sea environment.

5.2 Episode II: 17 January 2003

A detailed summary of the atmospheric circulation on 17 January is given in Taylor and Webb (2005). Passage of a broad frontal system deteriorated the fire conditions

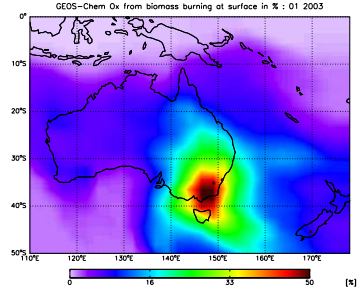

a.)

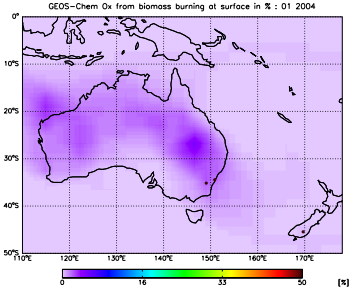

b.)

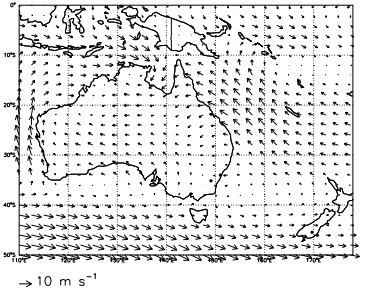

c.)

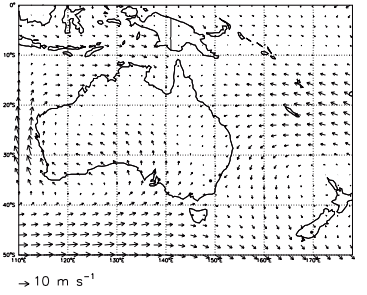

d.)

Fig. 4. Illustration of biomass burning sensitivity simulation: a.) and b.) Surface O_3 [%] in January 2003 and 2004. c.) and d.) Surface wind in January 2003 and 2004.

in NSW and fires in ACT spread rapidly under the influence of strong winds. On 18 January, the Forest Fire Danger Index (FFDI), an index used in Australia to assess the likelihood and severity of bushfires, reached 104. The ”extreme” fire danger index

episode	Date	Weather summary	Wind speed direction	MODIS
ES1	January 12	anti-cyclone NE of Tasmania	5 m/s E	partly
ES2	January 17	anti-cyclone Tasman sea	0-5 m/s N-NW	yes
ES3A	January 24-25	NW wind channel across Tasman sea	5-10 m/s N	yes
ES3B	January 26	NW wind channel across Tasman sea	5-15 m/s NW	yes
ES4	January 29	anti-cyclone Tasman sea	5-10 m/s N	yes

Table 2. Summary of bushfire episods January 2003. Column 1: Episode number. Column 2: Date. Column 3: Summary of the weather regime over south-east Australia. Column 4: Wind direction. Column 5: MODIS AOD signiture of the episode.

threshold is 50 or above. In fig. 6a strong winds in the range of 10 m/s (36 km/h) are seen close to Canberra (the inland dot on fig. 6a), but the frontal system is difficult to locate. The afternoon O_3 concentrations on 17 January in ACT, NSW and Vic are in the range 40 to 80 ppb. One EPA station in Vic reports an average O_3 of 89 ppb and 9 out of 15 stations report concentrations in the 40-80 ppb range. Note, the observed O_3 gradient in the metropolitan Sydney area. While the coastal stations report O_3 concentrations on average 20 ppb, the inland stations report 40-80 ppb (fig. 6b).

In fig. 6d, the observed AOD peaks over the Tasman Sea coastal area. It is to be noted that the AOD is a measure for the aerosol load in the entire troposphere thus reflecting the faster transport in the free troposphere and the slow down of the winds close to surface. The simulated AOD (fig. 6c) is in agreement with the satellite obser-

vation, but the model tends to underestimate the aerosol load over the Tasman Sea, which possibly reflects a known model weakness associated with parameterisation of the injection height during bushfires.

5.3 Episode III: 24-25 January 2003

On 25 January, a well-formed anti-cyclone over Tasman Sea is seen in fig. 7a. Over south-east Australia, the prevailing wind is from the north (N) and the wind speed is in the range 5-10 m/s. Note in addition a strong northerly flow east of Tasmania with wind speed reaching 16 m/s. In fig. 7b the surface O_3 enhancement reflects the wind flow and the simulated O_3 reaches 60 ppb over the Tasman Sea east of Tasmania. The observed O_3 in Victoria are in good agreement with the simulations, and it is to be noted that they range from 32-56 ppb. Once again the EPA observations in New South Wales show similar pattern to the reported in section 5.2, which probably reflects photochemical O_3 formation from anthropogenic sources. As mentioned before the metropolitan Sydney area is a closed basin, bounded by high-altitude escarpment to the south, west and north. During the fair weather summer afternoons, sea breeze conditions develop with light wind coming from the relatively cool water to the warm land. Those conditions favor the inland development of photochemical smog and can possibly explain the large west-east gradient. In addition the topography serves as a barrier for the atmospheric flow. Note, however, that a sea breeze circulation will be difficult to resolve with a coarse resolution model and will require a mesoscale model with a better temporal and spatial resolution.

A close investigation of MODIS AODs show aerosol enhancement of the order of 0.5 over Tasmania, the Tasman Sea and the South Island of New Zealand (fig. 7d). The simulated AOD confirms the enhancement over Tasmania and Tasman Sea but does not reach New Zealand (fig. 7c). Despite its patchy nature the observed high AODs hint to possible mid-tropospheric long range transport of bushfire smoke to New Zealand. This is further investigated below.

According to Taylor and Webb (2005), on 26 January 2003 the atmospheric circula-

tion is driven by a cold front with a pre-frontal trough moving east through south-east Australia. Well seen on fig. 8b is a strong NW wind channel across the Tasman Sea. Ahead of the wind channel is an anti-cyclone and behind it, at the point where the winds change to westerlies (W) east of Tasmania, is the cold front. The NW wind channel is a very efficient pathway for pollution transport and a similar pathway is reported over the North Atlantic by Guerova et al. (2006). Well seen in fig. 8a are high O_3 concentrations in the range 40-60 ppb across the Tasman Sea and west coast of New Zealand. The simulated AOD also suggests an increase over the Tasman Sea and the South Island of New Zealand. Note, however, that there appears to be a time lag between the model and MODIS observations with the observed AODs of 0.5 to the north of the simulated AODs. Due to the patchiness of MODIS data, it is difficult to draw a definite conclusion but it is very likely that the bushfire air reached the North Island of New Zealand on 26 January 2003. It is to be noted that on this day the bushfire reached the Sydney metropolitan area (fig. 8a) and after the frontal passage the O_3 dropped below 20 ppb in Victoria.

5.4 Episode IV: 29 January 2003

In a very similar weather situation to the one reported in section 5.3, with a blocking anti-cyclone over the Tasman Sea (fig. 9a) and cold front approaching Victoria on 29 January, the bushfire smoke reached the metropolitan area of Melbourne and the avarege surface O_3 incresed to 50 ppb from 20 ppb on January 27 (fig. 3). At 14 out of 15 stations the observed afternoon O_3 concentrations are in the range 40-80 ppb. The simulated surface O_3 peaks to the east of the metropolitan area of Melbourne (fig. 9a). The observed and simulated AOD peaks over the Bass Strait, between mailand Australia and Tasmania, and south-east coast of Australia (fig. 9c and d). Note, in addition, that close to the west coast of New Zealand the AOD reaches 0.5. On 30 January, similar NW channeling of the flow occurred across the Tasman Sea (not shown) but the wind speed was roughly doubled, i.e. 30 m/s and long range transport of O_3 and aerosols took place. The observed surface O_3 in Melbourne dropped rapidly

to 15 ppb after the frontal passage on 30 January.

5.5 Bushfire O_3 enhancement

The described change in the weather regime in section 5.3 and 5.4 driven by the passage of the cold front is an opportunity to quantify the contribution of the bushfires to the surface O_3 concentration over south-east Australia. As seen in fig. 3, in both episodes the observed surface O_3 peaks at 50 ppb before the frontal passage on 25 and 29 January and drops to 20 and 15 ppb after the frontal passage on 27 and 30 January, respectively. Thus, an increase of 35 and 30 ppb can be attributed to the bushfire. The model attributes 50 and 15 ppb O_3 increases due to bushfires during the two episodes. For the other two episodes on 12 and 17 January the observed surface O_3 peaks at 40 and 45 ppb correspondingly before dropping to 20 ppb. This gives 20 and 25 ppb enhancement due to bushfires. The average simulated enhancement is 40 and 25 ppb correspondingly. Based on the 4 episodes the range of observed O_3 enhancement over south-east Australia is 20-35 ppb which is a factor of 3 to 5 higher than the monthly mean of 6.5 ppb (table 1). The simulated O_3 enhancement is in the range 15-50 ppb with a factor of 1.5 to 5 higher than the monthly mean of 10 ppb. Despite the coarse model resolution and possible transport error associated with timeliness of frontal passage, GEOS-Chem is a backbone of this study and is a valuable tool in analysing the bushfire driven air quality. The ongoing development effort for multiple nesting of the model will allow extension of this analysis to the NSW region, which was excluded from this work due to consistent model overestimation driven by the topography and sea breeze circulation.

6 Summary and conclusions

The exceptionally severe 2002-2003 bushfire season in south-east Australia is closely related to the prolonged El Niño driven drought. The bushfires in south-east Australia

started in early January 2003 and the surface O_3 and aerosol loading roughly doubled when compared to January 2004. On 17, 24 and 25 January 2003 O_3 exceedences of the 1-hour (100 ppb) and 4-hour (80 ppb) standards are reported in Victoria, all due to the bushfires burning in Victoria and New South Wales. From model sensitivity simulations four episodes are identified, on 12, 17, 24-25 and 29 January 2003, during which the bushfires contribute by more that 10 ppb. These episodes are studied in detail in order to quantify the O_3 enhancement and the typical weather regimes.

During three episodes an anti-cyclone is located east of mainland Australia, over the Tasman Sea. On 26 and 30 January, a distinct surface wind channel is formed across the Tasman Sea between the anti-cyclone and the cold front behind it, through which the pollution crosses the Tasman Sea and reaches New Zealand. This type of long range pollution transport has been reported over the North Atlantic and its main characteristic is that it takes place on a short time span, i.e. few hours. The passage of the cold front resulted in a drop in surface O_3 and AOD over south-east Australia. This change from polluted to clean environments allows us to quantify the O_3 contribution due to bushfires. Based on the 4 episodes the range of observed O_3 enhancement due to bushfires is 20-35 ppb, which is a factor of 3 to 5 higher than the monthly mean of 6.5 ppb. The simulated bushfire O_3 enhancement is in the range 15-50 ppb with a factor of 1.5 to 5 higher than the monthly mean of 10 ppb. Note that the model exhibits very good skills in representing the temporal variation of the observed O_3 with the correlation of 0.81 but shows a tendency to overestimate the O_3 which is possibly linked to the relatively coarse resolution.

Both in January 2003 and 2004 high O_3 concentrations are simulated over central Australia. Careful examination of the weather regimes shows an anti-cyclonic flow curvature occurs over south-east Australia, between the Adelaide and Melbourne, which is a common feature in both 2003 and 2004 suggesting that central Australia is a receptor of the pollution from metropolitan Victoria and South Australia. In addition, a distinct O_3 enhancement is simulated north of Perth with prevailing southerly winds which suggests a possible advection from metropolitan area of Perth. Those findings

will be subject of a future work.

As expected an increase of the aerosol load occurred during January 2003 bushfires. Over south-east Australia and the Tasman Sea, during the four episodes the AOD reached 0.5 and the simulated and observed AODs agree well for the spatial structure. The model shows a tendency to underestimate the AOD, but proves a useful tool for reconstruction of the mostly patchy observed MODIS AODs. As the AODs represent the load in the troposphere it also reflects the faster transport in the free troposphere and the AOD enhancements are seen about a day ahead from the surface O_3 enhancement.

GEOS-Chem is a backbone of this study and is a valuable tool in analysing the bushfire driven air quality in south-east Australia. The model resolution is a limiting factor for application of this study to the Sydney basin. The ongoing development effort for multiple nesting of the model will allow extension of this analysis to the NSW region. In addition, a possible coupling of the GEOS-Chem Near-Real-Time (NRT) simulations (http://coco.atmos.washington.edu/cgi-bin/ion-p?page=geos_nrt.ion) with Sentinel (http://sentinel.ga.gov.au/acres/sentinel/), the national bushfire monitoring system, will provide a useful tool for chemical weather forecasting and nowcasting of the air quality during the bushfire season in Australia.

Acknowledgement

The GEOS-Chem is managed by the Atmospheric Chemistry Modeling Group at Harvard University with support from the NASA Atmospheric Chemistry Modelling and Analysis Program. We are grateful to the Australian Partnership for Advanced Computing (APAC) for resources and support; sensitivity experiments require indeed a lot of computing power! We would like to acknowledge the MODIS and NWS, Vic and SA EPA teams for providing observation data.

References

Abdou, W. A., Diner, D., Martonchik, J., Bruegge, C., Kahn, R., Gaitley, B., Crean, K., Remer, L., and Holben, B.: Comparison of coincident Multiangle Imaging Spectroradiometer and Moderate Resolution Imaging Spectroradiometer aerosol optical depths over land and ocean scenes containing Aerosol Robotic Network sites, JGR, 110,, D10S07, doi: 10.1029/2004JD004693, 2005.

Australia, E. S.: Ambient Air Quality Monitoring, South Australia, 19792003, Tech. rep., EPA South Australia, Adelaide, http://www.epa.sa.gov.au/pub_air.html, June 2004.

Auvray, M. and Bey, I.: Long-Range Transport to Europe: Seasonal Variations and Implications for the European Ozone BudgetA, J. Geophys. Res., 110, doi: 10.1029/2004JD005 503, 2005.

Benkovitz, C. M., Scholtz, M. T., Pacyna, J., Tarrasin, L., Dignon, J., Voldner, E. C., Spiro, P. A., Logan, J. A., and Graedel, T. E.: Global gridded inventories of anthropogenic emissions of sulfur and nitrogen., JGR, 101, doi:10.1029/96JD00 126, 1996.

Bey, I., Jacob, D. J., Logan, J. A., and Yantosca, R. M.: Global modeling of tropospheric chemistry with assimilated meteorology: Model description and evaluation, J. Geophys. Res., 106, 23.073–23.095, 2001.

Chin, M., Chu, A., Levy, R., Remer, L., Kaufman, Y., Holben, B., Eck, T., Ginoux, P., and Q.Gao: Aerosol distribution in the Northern Hemisphere during ACE-Asia: Results from global model, satellite observations, and Sun photometer measurements, JGR, 109, D23S90, doi: 10.1029/2004JD004829, 2004.

Giglio, L., van der Werf, G. R., Randerson, J. T., Collatz, G. J., and Kasibhatla, P.: Global estimation of burned area using MODIS active ?re observations, Atmos. Chem. Phys., 6, 957–974, 2006.

Guenther, A., Karl, T., Harley, P., Wiedinmyer, C., Palmer, P., and Geron, C.: Estimates of global terrestrial isoprene emissions using MEGAN (Model of Emissions of Gases and Aerosols from Nature), Atmos. Chem. Phys., 6, 3181–3210, 2006.

Guerova, G., Bey, I., Attie, J.-L., Martin, R. V., Cui, J., and Sprenger, M.: Impact of transatlantic transport episodes on summertime ozone in Europe, Atmos. Chem. Phys., 6, 2057–2072, 2006.

Gupta, P., Christopher, S. A., Wang, J., Gehrigc, R., Leed, Y., and Kumare, N.: Satellite remote sensing of particulate matter and air quality assessment over global cities, Atmos. Env., 40,

5880–5892, doi:doi:10.1016/j.atmosenv.2006.03.016, 2006.
Gupta, P., Christopher, S. A., Box, M., and Box, G.: Multi year satellite remote sensing of particulate matter air quality over Sydney, Australia, Int. J. Remote Sensing, 28:20, 16, doi: 10.1080/01431160701241738, 2007.
Hennessy, K., Lucas, C., Nicholls, N., Bathols, J., Suppiah, R., and Ricketts, J.: Climate change impacts on fire-weather in south-east Australia, Tech. rep., CSIRO Marine and Atmospheric Research Aspendale Victoria, 2005.
Ichoku, C., Chu, D., Mattoo, S., Kaufman, Y., Remer, L., Tanre, D., Slutsker, I., and Holben, B.: A spatio-temporal approach for global validation and analysis of MODIS aerosol products, Geophys. Res. Lett., 29, doi:10.1029/2001GL013206, 2002.
Jacob, D. J.: Introduction to Atmospheric Chemistry, Princeton University Press, http://www.as.harvard.edu/people/faculty/djj/book/index.html, 1999.
King, M. D., Kaufman, Y. J., Menzel, W. P., and Tanreacute, D.: Remote sensing of cloud, aerosol, and water vapor properties from the Moderate Resolution Imaging Spectrometer (MODIS), IEEE Transactions on Geoscience and Remote Sensing, 30, 2–27, 1992.
King, M. D., Menzel, W. P., Kaufman, Y. J., Tanre, D., Gao, B.-C., Platnick, S., Ackerman, S. A., Remer, L. A., Pincus, R., and Hubanks, P. A.: Cloud and aerosol and water vapor properties, precipitable water, and profiles of temperature and humidity from MODIS, IEEE Transactions Geoscience and Remote Sensing, 41, 442–458, 2003.
Kinne, S.: Monthly averages of aerosol properties: A global comparison among models, satellite data, and AERONET ground data, J. Geophys. Res., 108, 4634, doi:10.1029/2001JD001253, 2003.
Leslie, L. M. and Speer, M. S.: Modelling dust transport over central eastern Australia, Meteorol. Appl., 13, 141–167, doi:10.1017/S1350482706002155, 2006.
Levy, C. R., Remer, L., Martins, J., Kaufman, Y., Plana-Fattori, A., Redemann, J., and Wenny, B.: Evaluation of MODIS Aerosol Retrievals over Ocean and Land during CLAMS, J. Atmos. Sci., 62, 974–992, 2005.
Liu, H., Jacob, D. J., Bey, I., Yantosca, R. M., Duncan, B. N., and Sachse, G. W.: Transport pathways for Asian pollution outflow over the Pacific: Interannual and seasonal variations, J. Geophys. Res., 108, 8786, 2003.
Manins, P.: Australia State of the Environment Report 2001, Tech. rep., Environmental Consulting and Research Unit, CSIRO Atmospheric Research, Aspendale Victoria, iSBN 0 643 06746 9, 2001.

Martin, R. V., Jacob, D., Yantosca, R., Chin, M., and Ginoux, P.: Global and Regional Decreases in Tropospheric Oxidants from Photochemical Effects of Aerosols, J. Geophys. Res., 108, doi: 10.1029/2002JD002 622, 2003.

Matsui, T., Kreidenweis, S., Sr., R. P., Schichtel, B., Yu, H., Chin, M., Chu, D., and Niyogi, D.: Regional comparison and assimilation of GOCART and MODIS aerosol optical depth across the eastern U.S., Geophys. Res. Lett., 31, L21 101, doi:10.1029/2004GL021017, 2004.

Mitchell, R. M., O'Brien, D. M., and Campbell, S. K.: Characteristics and radiative impact of the aerosol generated by the Canberra firestorm of January 2003, JGR, 111, D02 204, 10.1029/2005JD006304, 2006.

Park, R., Jacob, D. J., Field, B. D., Yantosca, R. M., and Chin, M.: Natural and transboundary pollution influences on sulfate-nitrate-ammonium aerosols in the United States: Implications for policy, J. Geophys. Res., 109, 10.1029/2003JD004 473, 2004.

Remer, L. A.: Validation of MODIS aerosol retrieval over ocean, Geophys. Res. Lett., 29(12), 8008, doi:10.1029/2001GL013204, 2002.

Salomonson, V. V., Barnes, W. L., Maymon, P. W., Montgomery, H. E., and Ostrow, H.: MODIS: Advanced facility instrument for studies of the earth as a system, IEEE Transactions on Geoscience and Remote Sensing, 27, 145–153, 1989.

Streets, D. G., Bond, T., Carmichael, G., Fernandes, S., Fu, Q., Klimont, Z., Nelson, S., Tsai, N., Wang, M., Woo, J.-H., and Yarber, K. F.: An inventory of gaseous and primary aerosol emissions in Asia in the year 2000, J. Geophys. Res, 108, doi:10.1029/2002JD003 093, 2003.

Streets, D. G., Zhang, Q., Wang, L., He, K., Hao, J., Wu, Y., Tang, Y., and Carmichael, G.: Revisiting China's CO emissions after the Transport and Chemical Evolution over the Pacific (TRACE-P) mission: Synthesis of inventories, atmospheric modeling, and observations, J. Geophys. Res, 111, doi:10.1029/2006JD007 118, 2006.

Taylor, J. and Webb, R.: Meteorological aspects of the January 2003 south-eastern Australia bushfire outbreak, Australian Forestry, 68, 94–103, 2005.

van der Werf, G., Randerson, J., Giglio, L., Collatz, G., Kasibhatla, P., and Arellano, A.: Interannual variability in global biomass burning emissions from 1997 to 2004, Atmos. Chem. Phys., 6, 3423–3441, 2006.

Victoria, E.: Air Monitoring Report 2003 - Compliance with the National Environment Protection (Ambient Air Quality) Measure, Tech. rep., EPA Victoria, Melbourne, http://www.epa.vic.gov.au/air/monitoring/air_monitoring_report_2003.asp, June 2004.

Wang, Y., Jacob, D., and Logan, J.: Global simulation of tropospheric ozone-NO_x-Hydrocarbon chemistry, J. Geophys. Res., 103, 10,713–10,768, 1998.
Wesely, M.: Parameterization of surfaceresistance to gaseous dry deposition in regional-scale numerical models, Atmos. Environ., 23, 1293–1304, 1989.
Wild, O. and Akimoto, H.: Intercontinental transport of ozone and its precursors in a three-dimensional global CTM, J. Geophys. Res., 106, 10.1029/2000JD000 123, 2001.
Yienger, J. J. and Levy, H.: Empirical model of global soil-biogenic NOx emissions, J. Geophys. Res., 100, 11 447 – 11 464, 1995.

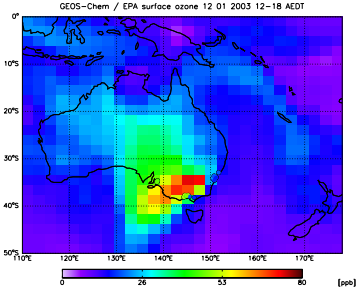

a.)

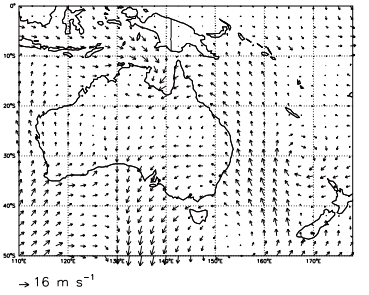

b.)

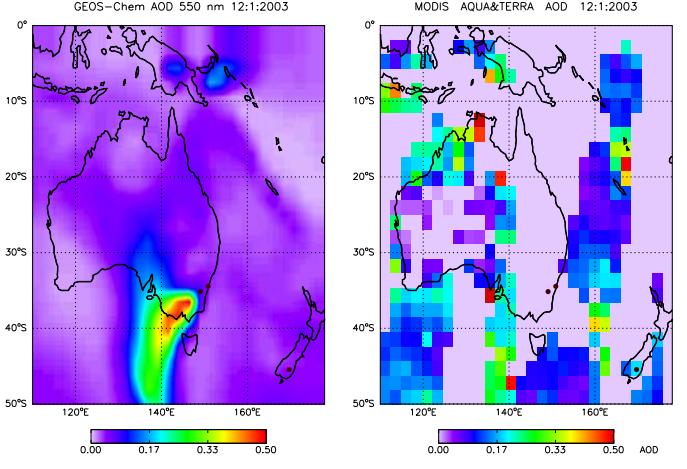

c.)

Fig. 5. a.) GEOS-Chem surface O_3: 12 January 2003. b.) GEOS-Chem surface wind. c.) and d.) GEOS-Chem and MODIS AODs: 12 January 2003.

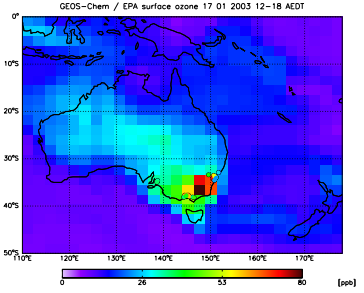

a.)

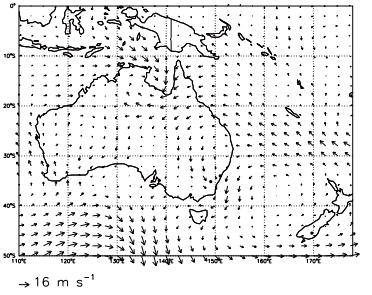

b.)

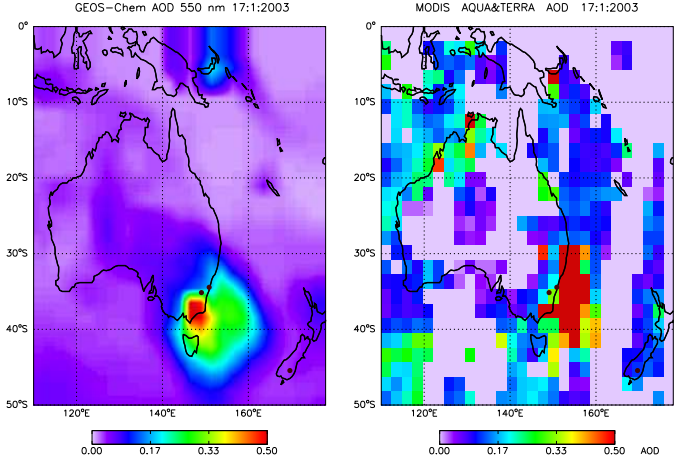

c.)

Fig. 6. a.) GEOS-Chem surface O_3: 17 January 2003. b.) GEOS-Chem surface wind. c.) and d.) GEOS-Chem and MODIS AODs: 17 January 2003.

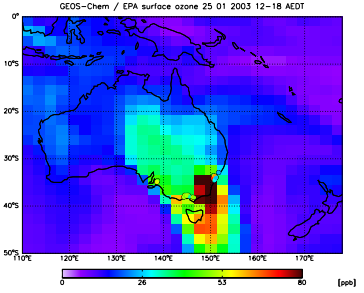

a.)

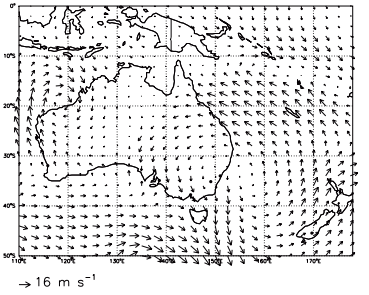

b.)

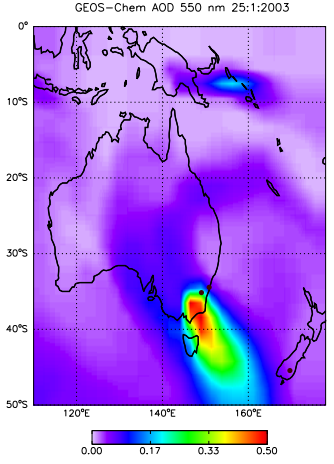

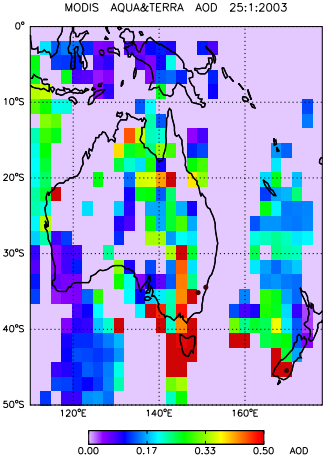

c.)

Fig. 7. a.) GEOS-Chem surface O_3: 25 January 2003. b.) GEOS-Chem surface wind. c.) and d.) GEOS-Chem and MODIS AODs: 25 January 2003.

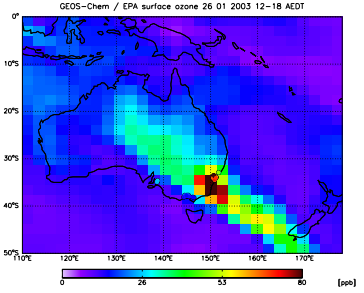

a.)

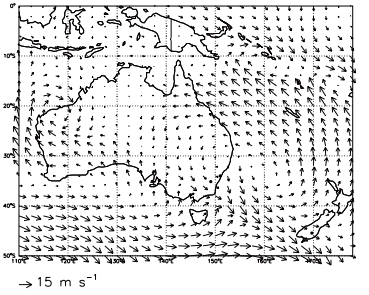

b.)

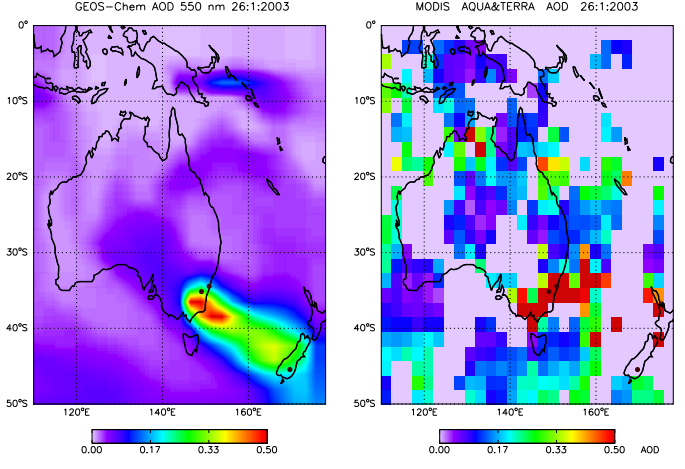

c.)

Fig. 8. a.) GEOS-Chem surface O_3: 26 January 2003. b.) GEOS-Chem surface wind. c.) and d.) GEOS-Chem and MODIS AODs: 26 January 2003.

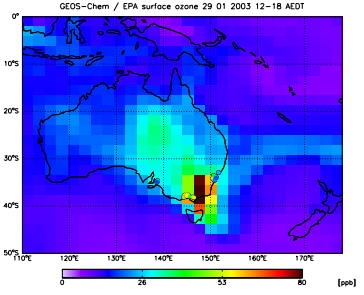

a.)

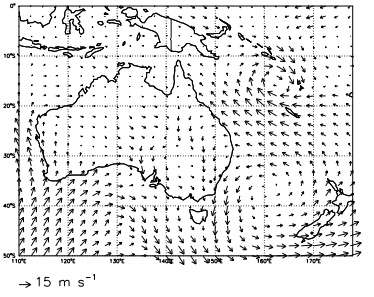

b.)

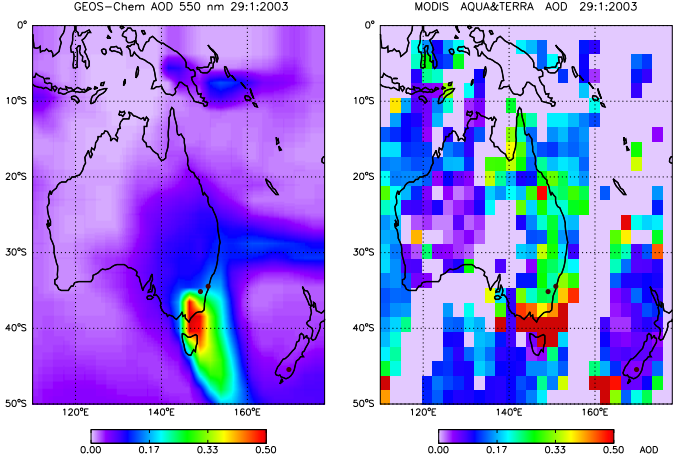

c.)

Fig. 9. a.) GEOS-Chem surface O_3: 29 January 2003. b.) GEOS-Chem surface wind. c.) and d.) GEOS-Chem and MODIS AODs: 29 January 2003.